

## Subsidence history of the north Indian continental margin, Zaskar–Ladakh Himalaya, NW India

R. I. CORFIELD<sup>1,2</sup>, A. B. WATTS<sup>1</sup> & M. P. SEARLE<sup>1</sup>

<sup>1</sup>Department of Earth Sciences, Oxford University, Parks Road, Oxford OX1 3PR, UK (e-mail: tony@earth.ox.ac.uk)

<sup>2</sup>Present address: BP Exploration, Farburn Industrial Estate, Dyce, Aberdeen AB21 7PB, UK

**Abstract:** Detailed geological field mapping has allowed the restoration of two full stratigraphic sections through the highly deformed Mesozoic and Early Tertiary fold and thrust belt of the north Indian continental margin. The two sections, which are representative of a proximal and a distal facies on the margin, have been backstripped using standard techniques. Profiles of the tectonic subsidence and uplift through the pre-collisional history of the margin have been constructed and compared with the predictions of simple thermal and mechanical models. The pre-collisional history can be explained by a thermal model with an initial age of rifting of 270 Ma and a stretching factor,  $\beta$ , of *c.* 1.2. This model accounts for the general exponential decrease in the backstripped tectonic subsidence. The model fails, however, to completely explain the subsidence and uplift history of the margin since the late Cretaceous. The history during this time is characterized by uplift at the most proximal location and an increase in subsidence at the most distal location. We attribute these differential vertical movements to flexural loading of the north Indian margin by obduction of the Spontang ophiolite. The best fit model is one in which a 70 km wide wedge-shaped load, tapering from 10 to 0 km thick, is emplaced on rifted lithosphere with an elastic thickness,  $T_e$ , of 5–10 km. These results, which are in accord with the late Cretaceous timing of obduction and the structure of the Spontang ophiolite, provide new constraints on the  $T_e$  structure of extended continental lithosphere 120–150 Ma after a rifting event.

**Keywords:** Himalaya, continental margin, backstripping, flexure, ophiolites.

The tectonic subsidence and uplift history of a sedimentary basin constrain the vertical movements that have modified it during geological time. Backstripping techniques applied to modern basins such as those in passive margin settings have been remarkably successful in determining the pattern of the tectonic subsidence and uplift. There have been comparatively few applications of these techniques, however, to highly deformed margins in the rock record.

In the Zaskar–Ladakh Himalaya, NW India (Fig. 1), the Spontang ophiolite is a thrust slice of oceanic crust and upper mantle that lies at present structurally above a continental margin carbonate sequence and its neo-autochthonous early Tertiary limestone cover. Controversy exists as to whether the ophiolite was obducted onto the northern passive margin of the Indian plate during the Eocene (Keleman & Sonnenfeld 1983; Reuber 1986; Colchen *et al.* 1987) or during the late Cretaceous (Searle 1986; Searle *et al.* 1988, 1997; Corfield & Searle 2000; Corfield *et al.* 2001).

The Spontang ophiolite was formed at  $177 \pm 1$  Ma (mid-Jurassic), as suggested by the U–Pb zircon age of diorite segregations in high-level gabbros (Pederson *et al.* 2001). An andesitic island arc sequence above the Spontang ophiolite basalts was dated at  $88 \pm 5$  Ma, which constrains the minimum age of subduction beneath the ophiolite. Structural studies and detailed mapping around the ophiolite have shown that a major phase of folding affected all Mesozoic units of the margin shelf sequence before deposition of the unconformably overlying Palaeocene–Eocene limestones (Searle 1986; Searle *et al.* 1988, 1997; Corfield & Searle 2000). Following the early Eocene (*c.* 50 Ma) collision between India and Asia, a renewed thrusting event placed the Spontang ophiolite over these limestones.

Previous studies, using estimates of subsidence rates for given

stratigraphic intervals of the Zaskar passive margin, suggest the timing of ophiolite obduction as either in the late Cretaceous (Searle 1986; Corfield & Searle 2000) or in the Eocene (Garzanti *et al.* 1987; Premori Silva *et al.* 1991). Gaetani & Garzanti (1991) presented a geohistory analysis for the passive margin sequence, but included no discussion of the assumptions and uncertainties involved. This paper presents the first attempt to quantitatively derive the tectonic subsidence and uplift history of the north Indian continental margin throughout its entire history, from the rifting and passive margin formation in the late Palaeozoic to the time of last marine sedimentation in the Eocene. We use these tectonic movements to better constrain the timing of ophiolite obduction and the thermal and mechanical structure of the north Indian continental margin.

### Stratigraphy

We have used in this study stratigraphic sections that have been compiled from field mapping across a highly deformed and eroded terrain. Restoration of the post-depositional structural evolution is therefore required so that stratigraphic units can be placed in their correct relative palaeogeographical positions. Furthermore, the construction of a stratigraphic section through the entire Mesozoic sequence (e.g. Fig. 2) requires data from exposures covering a sizeable area. The detailed summary of the stratigraphy given by Gaetani & Garzanti (1991) and the map and restorations presented by Corfield & Searle (2000) can be used for this purpose.

The Permian–Mesozoic shelf carbonate succession exposed in the Zaskar Range extended northward to the time-equivalent passive margin and slope deposits (Lamayuru complex) and

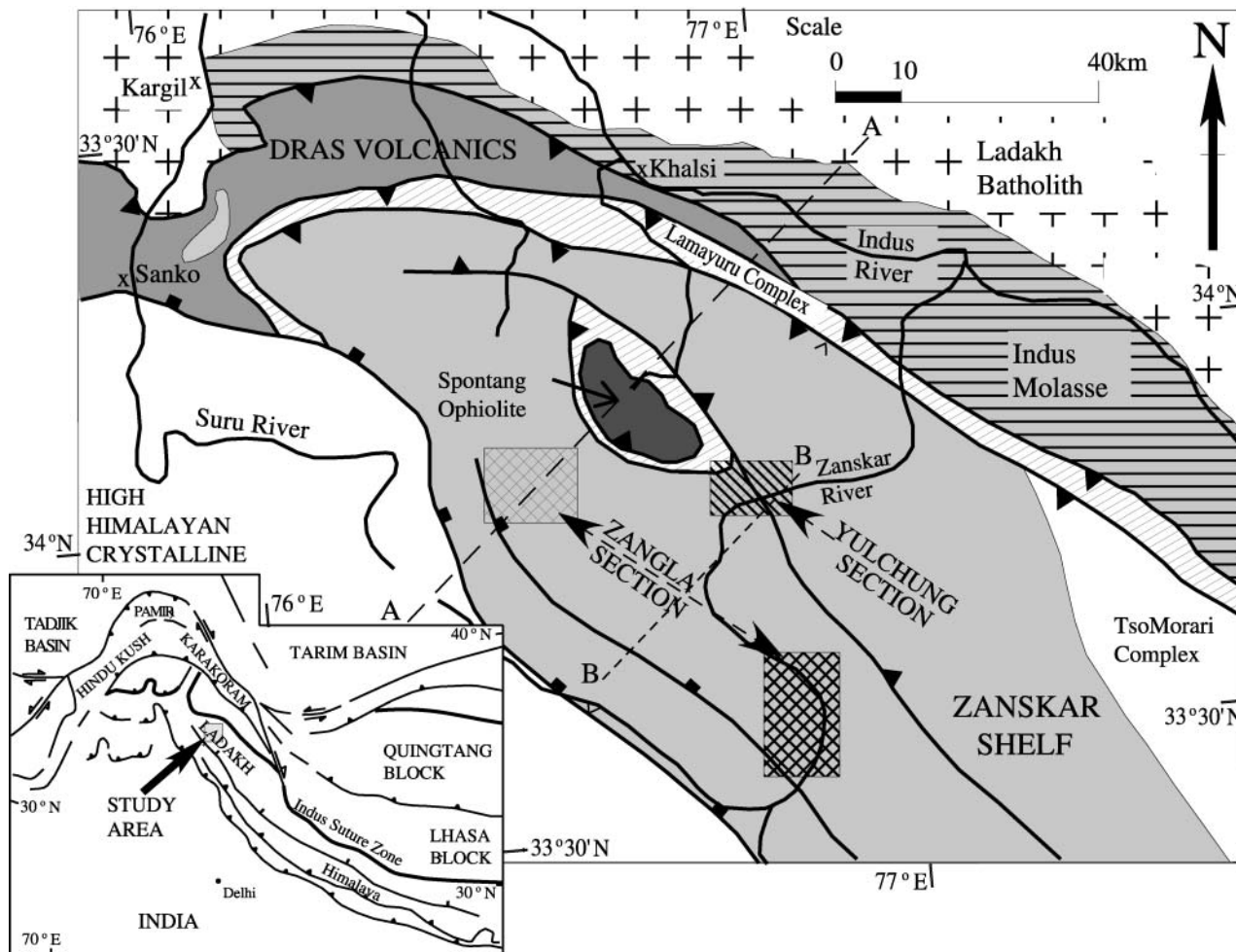


**Fig. 1.** Geological summary map of the Zaskar Himalaya showing the outcrop of the north Indian continental margin shelf sediments and the map extent of the areas used to compile the stratigraphic sections in this study. To the NW, the Lamayuru Formation represents the distal outer margin slope deposits and the edge of the Indus Suture Zone. To the south, the High Himalayan Crystalline sequence comprises metamorphosed passive margin sediments that have been exhumed between the Main Central Thrust and the Zaskar Shear Zone. Dashed lines indicate the location of sections A and B in Figure 3. Inset map shows the location in NW India.

further outboard to the distal, deep-water, Karamba complex (Robertson & Sharp 1988).

Figure 3, Section A, shows a full crustal-scale cross-section through the north Indian continental margin. A full discussion of the structure of this cross-section has been given by Corfield & Searle (2000). The figure also shows a more localized cross-section (Section B) along the Zaskar river illustrating the relative position of the two restored stratigraphic sections at Zangla and Yulchung.

To constrain the spatial variation in tectonic subsidence across the north-facing Indian margin two, or ideally more, stratigraphic sections are required. Because of considerable deformation at its most distal location and High Himalayan deformation and metamorphism at its southern, most proximal location, only a limited width of exposure remains, across which reasonably well-constrained sections can be constructed. However, excellent exposure in addition to large topographic variation means that the entire stratigraphic thickness can be restored using outcrops from a relatively restricted area. Consequently, it has been possible to compile two stratigraphic sections from the Singe–Yulchung–Nerak region and from the lower Zangla unit along

the Oma Chu and Zaskar valleys. The stratigraphic data for each section are summarized in Table 1.

Section 1 (Zangla section) from the Lower Zangla unit represents the most proximal parts of the continental margin for which the full sequence into the Eocene remains preserved. To construct a full section from the Permian to Eocene stratigraphy it was necessary to use outcrops from large distances along the strike of the passive margin (NW–SE), to minimize the proximal to distal variation incorporated into the section. This section restores to a pre-deformation position *c.* 30–40 km SW of section 2 (Corfield & Searle 2000).

Section 2 (Yulchung section) from the Singe–Yulchung–Nerak region in the hanging wall of the Photoksar break-back thrust is the most distal part of the continental margin unaffected by the  $D_3$  deformation (Searle 1986). In addition, the Zaskar river cuts a deep section through the stratigraphy, exposing the complete sequence from the Triassic to the Eocene within a small area. To complete the Yulchung section it was necessary to include data from the Permo-Triassic sequence in the southern Zaskar valley, which is not exposed further north. Consequently, the data used for the basal part of each section are the same.

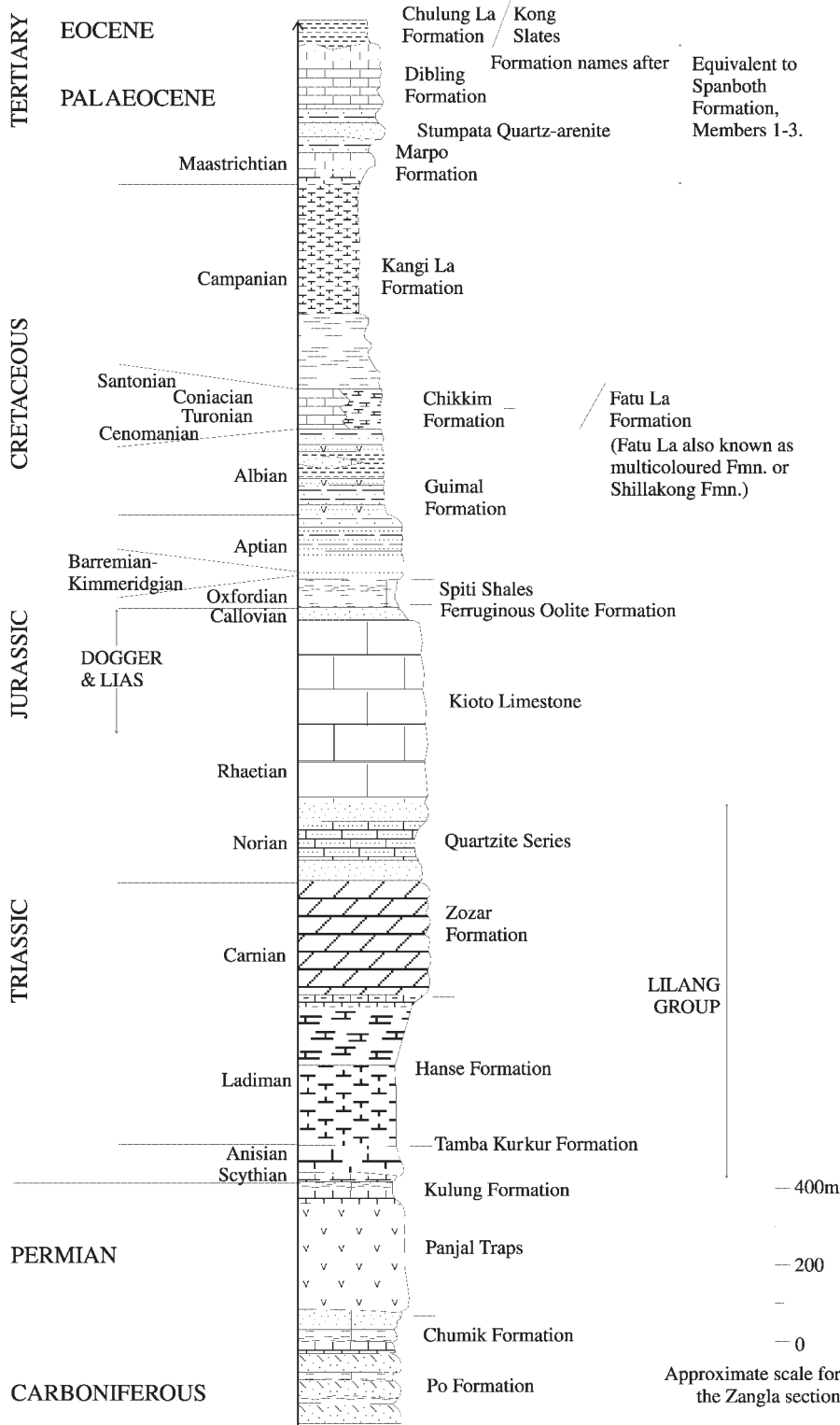


Fig. 2. Summary stratigraphic column for the Zanskar passive continental margin. Modified from Gaetani & Garzanti (1991) and references therein.

**Backstripping**

The restored stratigraphic sections of the Zanskar margin were backstripped using standard methods (e.g. Watts & Ryan 1976). For decompaction, we used the empirically derived porosity–depth curves for different lithologies given by Bond & Kominz (1984). It is notable that the uncertainty in the porosity range of

a single lithology at any given depth is not significantly greater than the uncertainty in porosity regardless of lithology. Only sand and shale at very shallow depths have porosity ranges that do not overlap. We therefore used a single porosity–depth relationship to decompact the entire section, regardless of lithology, on the basis that such a simple approach allows a more transparent evaluation of the results.



**Table 1.** Summary of stratigraphic data used to backstrip the restored sections at Zangla and Yulchung

Stratigraphic unit	Age at base (Ma)	Thickness (m)		Deposition depth (m)	
		Maximum estimate	Minimum estimate	Base of unit	Top of unit
<i>Zangla section</i>					
Top of section	45	–	–	–	–
Chulung La Formation	54	300	200	20	0
Dibling Limestone	63	210	150	50	20
Stumpata Quartzarenite	66	30	10	20	0
Marpo Limestone	74	140	80	30	20
Kangi La Formation	83	600	400	300	100
Chikkim Formation	91	90	90	400	300
Guimal Sandstone	132	430	300	100	10
Spiti Formation	154	100	20	100	50
Ferruginous Oolite Formation	159	35	20	30	10
Kioto Formation	218	500	450	100	20
Quartzite Series	224	250	150	30	10
Zozar Formation	231	350	200	50	20
Hanse Formation	240	450	400	200	50
Tamba Kurkur Formation	253	110	70	200	100
Kulung Formation	260	60	50	100	20
Panjal Traps	270	300	300	–	–
Total		3955	2890		
<i>Yulchung section</i>					
Top of section	45	–	–	–	–
Kong Slates	54	300	200	20	10
Kesi Limestone	58	160	140	20	10
Singe Limestone	63	220	200	100	50
Stumpata Quartzarenite	66	70	70	20	10
Marpo Limestone	74	30	10	100	50
Kangi La Formation	83	1100	900	300	200
Fatu La Formation	91	200	150	400	200
Guimal Sandstone	132	250	100	100	20
Spiti Formation	154	20	0	100	50
Ferruginous Oolite Formation	159	20	10	30	10
Laptal Formation	172	50	10	100	50
Kioto Formation	218	700	500	100	20
Quartzite Series	224	200	150	30	10
Zozar Formation	231	350	200	50	20
Hanse Formation	240	450	400	200	50
Tamba Kurkur Formation	253	110	70	200	100
Kuling Formation	260	60	50	100	20
Panjal Traps	270	300	300		
Total		4590	3460		

The age of each unit within the column forms a fundamental reference point in the calculated subsidence history. Any uncertainty in the horizon age can therefore be directly evaluated with reference to a tectonic subsidence v. age plot. Age determinations are based on those of Gaetani & Garzanti (1991).

The thickness of sedimentary units between the horizons is subject to uncertainty given the considerable extent of deformation suffered by the Zanskar shelf. Internal thickening of units is

common and can be very difficult to evaluate, particularly in the shaly units that deform on the large scale in a ductile manner. For these units, in particular the Kangi La Formation and the Kong Slates, area balancing of cross-sections has been used to provide estimates of the thickness. A range in the thickness estimate has been given in each case, which encompasses both observed lateral variation in stratigraphic thickness and measurement uncertainty.

The depth of deposition is generally constrained by the sedimentary environment of deposition for each unit, although direct palaeontological indicators are used wherever possible. In particular, assemblages of benthic Foraminifera can be compared with present-day bathymetric distributions of the same genera to provide an estimate of water depth. For shallow-water sediments the range of possible deposition depths is relatively small in comparison with deeper water deposits, for which the uncertainty can be of the order of 100 m, particularly where fossil evidence is absent. This major source of uncertainty is modelled in each case with a range of input values. The uncertainty in the depth of deposition has a direct effect on the subsidence inferred for a given stratigraphic interval but will not propagate to estimates for subsequent intervals.

The final uncertainty in backstripping is the choice of a suitable sea-level curve. Fluctuations in sea level have a direct effect on the calculated subsidence as sea level is the horizontal reference for the calculations. Three sea-level curves have therefore been used for these calculations (Pitman 1978; Watts & Steckler 1979; Haq *et al.* 1987) to ascertain the effect they have on the main interpretations.

### Evaluation of uncertainties

**Decompaction.** Figure 4a illustrates the results of backstripping the Yulchung section using shale maximum and sandstone minimum porosity–depth profiles. The overall subsidence varies by *c.* 20%, which is in good agreement with error estimates (Wooler *et al.* 1992) in other deformed margins. The effect of the porosity–depth relationship on the subsidence calculated is at its greatest in the middle of the stratigraphic section. However, in addition to having an effect on the overall subsidence, relative subsidence between two horizons will also be affected. For example, a shale at depth in the stratigraphic column, decompacted using a sand porosity–depth relationship, is likely to have its original porosity and thickness underestimated (although the empirically derived ranges do overlap). This would result in the underestimation of the tectonic subsidence that occurred during the deposition of the shales. The quantitative impact of such uncertainties is considered in the analysis of the results.

**Stratigraphic thickness.** Figure 4b illustrates the results of backstripping sections based on the maximum and minimum estimates of sediment thicknesses in addition to the best estimates. Once again, there is *c.* 20% variation in the overall subsidence between the maximum and minimum values. As a result of the complex structural history, the error in the thickness estimates may be variable from unit to unit. The best estimates in adjacent units could be respectively overestimated and underestimated. The implication once again is that the relative subsidence between two horizons may be significantly affected, although the overall subsidence could remain unaffected. The potential qualitative impact of the uncertainty has been considered in the interpretation of the results.

**Sea-level variation.** Although sea level has undoubtedly changed throughout time, the amplitude and wavelength of these fluctuations is disputed. Using sequence stratigraphic concepts applied to rift-type basins in passive margins, as well as other tectonic settings, Vail *et al.* (1977) and more recently Haq *et al.* (1987) have argued that global sea level is oscillatory with changes of up to 600 m. The Haq *et al.* (1987) curve integrates the most recent geochronological, magneto-stratigraphic and biostratigraphic data to provide a chronostratigraphic framework to which

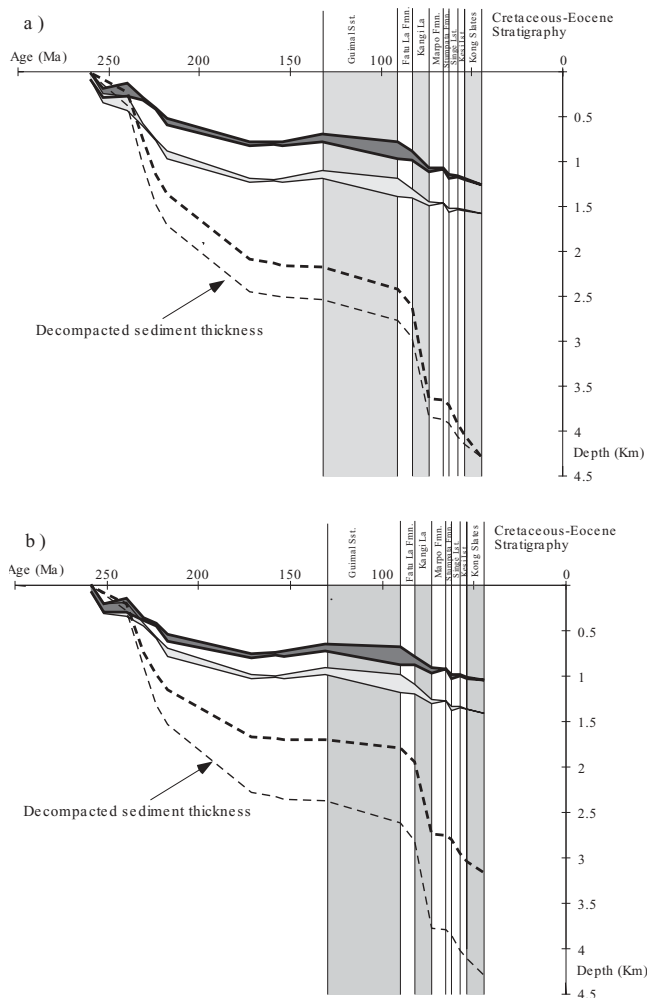


**Fig. 4.** Tectonic subsidence for the Yulchung section. (a) Calculated for end-member porosity–depth profiles. The bold curves were backstripped using a sandstone minimum porosity–depth profile; the fine lines using a shale maximum porosity–depth profile. The shaded region between the curves indicates the uncertainty arising from the depth of deposition (i.e. palaeobathymetry). The bold dashed line is the current sediment thickness. The fine dashed line is the decompacted sediment thickness. (b) Calculated from the maximum (fine lines) and minimum (bold lines) estimates for the thickness of the stratigraphic formations. Shading as in (a).

depositional sequences are tied. The long-wavelength component of the Haq *et al.* (1987) curve is very similar to the Pitman (1978) curve. However, others have pointed out that it is essential to allow for the effects of tectonic movements within the basins studied when constructing these curves (Watts & Steckler 1979). This approach leads to smoother sea-level variation curves of lower amplitude.

To compare the effect of the sea-level curve on the tectonic subsidence estimates, we have used three curves to backstrip the Zangla and Yulchung sections. The magnitude of variation introduced is directly compared in Figure 5. The Watts & Steckler (1979) curve is largely subparallel to the Haq *et al.* (1987) curve. The Pitman (1978) curve, however, shows a significant deviation in trend from the other curves during the Cretaceous.

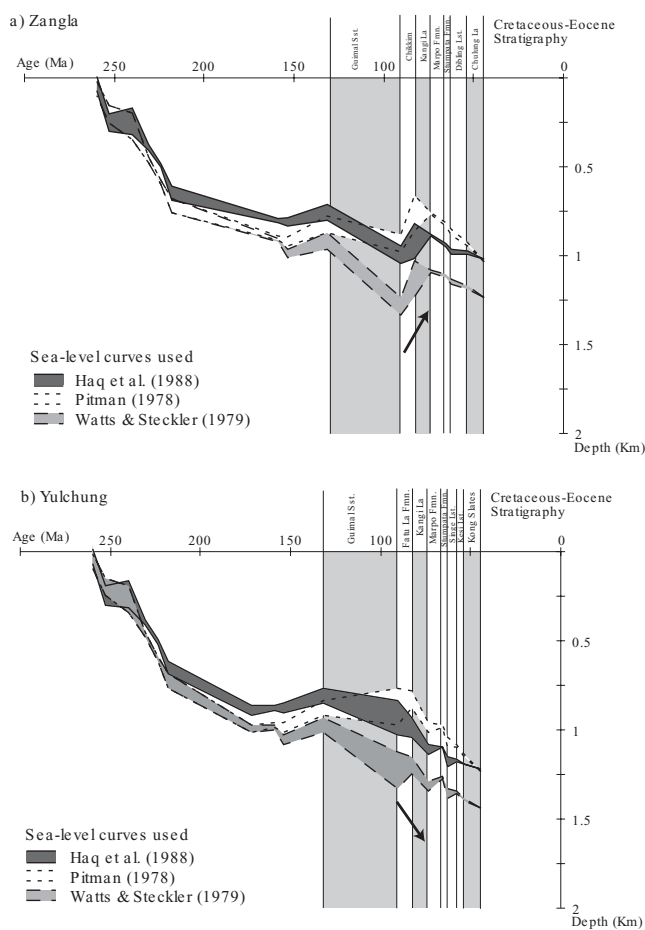


**Fig. 5.** Comparison of (a) the Zangla and (b) the Yulchung section backstrip using different estimates of sea level. The sections backstripped use the best estimates for stratigraphic thickness and the shale minimum porosity–depth relationship. The bold arrows indicate the uplift and subsidence ‘event’ that affects the Zangla and Yulchung sections respectively and has been attributed to ophiolite obduction.

## Results

### Passive margin stage

Figure 6a–c illustrates the results of backstripping each of the sections using the best estimates for the stratigraphic thicknesses and different sea-level curves. The most striking feature of the resulting subsidence profiles is the exponential form of the curves between 260 Ma at the base of the section and 130 Ma. The curves appear to conform well to the predictions of the stretching models of McKenzie (1978) and Jarvis & McKenzie (1980).

A rough estimate of the amount of stretching experienced at the location of each of the sections can be obtained by isostatic balancing of crustal columns before and after stretching. We then obtained:

$$\beta = \frac{(\rho_m - \rho_c)t_c}{(\rho_m - \rho_c)t_c - Y(\rho_m - \rho_w)}$$

where  $\beta$  is the stretching factor,  $t_c$  is the initial crustal thickness,  $Y$  is the total tectonic subsidence, and  $\rho_m$ ,  $\rho_w$  and  $\rho_c$  represent the density of mantle, water and crust, respectively. Assuming  $t_c = 31.2$  km and  $Y = 0.80$  km for the Zangla section and

$t_c = 31.2$  km and  $Y = 0.85$  km for the Yulchung section (at 150–100 Ma), the best fit  $\beta$  is 1.13 and 1.14, respectively. However, these values are likely to be underestimates, as they are based on the sedimentary sequence following the syn-rift. Panjal volcanic series. The pre-rift topography and elevation above sea level, in addition to the intrusive and extrusive thickness of the synrift basalts, may accommodate extra subsidence before the onset of deposition of the backstripped section.

To obtain a more accurate estimate of  $\beta$ , the model of Jarvis & McKenzie (1980) has been used to generate theoretical subsidence curves that have been fitted to the data from the backstripped sections (Fig. 6a–c). The estimated age at the base of the Panjal volcanic series (270 Ma; Gaetani *et al.* 1990) was assumed to mark the onset of the rifting stage.

The calculated tectonic subsidence curves in Figure 6 consist of two parts, the initial syn-rift subsidence and the exponential post-rift thermal subsidence. The exponential decay in the rate of thermal subsidence is only weakly dependent on the duration of stretching (Cochran 1983). Consequently, the exponential can be fitted to theoretical curves by varying only the  $\beta$  and crustal thickness values. For each section, 220 Ma appears to mark the onset of the exponential post-rift thermal subsidence, giving an estimate for the duration of stretching of 270 Ma – 220 Ma, i.e. 50 Ma. This value is similar to that found for Tethyan margins of the Alpine region (Wooler *et al.* 1992).

The total subsidence is sensitive to the initial crustal thickness as well as to the  $\beta$  value. The value of  $t_c = 31.2$  km that we have assumed is a typical one for zero elevation, isostatically balanced, continental crust (Cochran 1981). However, an equally good fit could have been obtained for slightly lower and higher crustal thicknesses with corresponding higher and lower  $\beta$  values, respectively.

The Watts & Steckler (1979) sea-level curve (Fig. 6b) gives a good overall fit to the smooth exponential decay in the rate of subsidence with a best estimate of  $\beta$  of 1.19 and 1.20 for the Zangla and Yulchung sections, respectively. The Haq *et al.* (1987) curve (Fig. 6a) also gives a good fit to exponential decay with slightly lower  $\beta$  estimates. The Pitman (1978) curve (Fig. 6c) gives the worst overall fit to exponential subsidence of the three curves and it is likely, we believe, that the magnitude of sea level for the Cretaceous is considerably overestimated in this case.

The similarity in the  $\beta$  values obtained for the Yulchung and Zangla sections probably reflects relatively uniform extension over the part of the shelf covered by these sections. However, the slightly higher value for the more distal section of the passive margin conforms with expectations.

For several reasons, these values of  $\beta$  are likely to be underestimates. Airy isostasy has been assumed for the purposes of backstripping. However, the existence of a finite strength crust means a smaller contribution of sedimentary loading and, hence, a larger contribution of the tectonic subsidence and uplift.

The generation of a significant volume of melt during stretching will also cause  $\beta$  to be underestimated. This is because magmatic material thickens the crust, creating uplift rather than subsidence. The presence of extrusive volcanic rocks during the rifting stages (Panjal Traps) suggests that a large volume of melt may also have been added to the crust intrusively. The alkalic to tholeiitic compositions of the extrusive rocks (Honegger *et al.* 1982) suggest a large melt volume associated with rifting. Given a high mantle potential temperature of 1480 °C the melt compositions are consistent with a  $\beta$  value of 2.0 (McKenzie & Bickle 1988). More typical, lower-mantle potential temperatures would require an even higher  $\beta$  value to account for the melt



compositions. Similar processes have been invoked for the North Atlantic passive margin of SE Greenland related to high asthenospheric temperatures associated with the Iceland plume (Clift *et al.* 1995).

#### *Early Cretaceous*

The smooth exponential form of the subsidence curves based on the Watts & Steckler sea-level curve (Fig. 6b) is broken during the early Cretaceous by a slight but significant increase in the subsidence rate. This apparent subsidence may be due, at least in part, to an overestimate of the deposition depth for the Chikkim limestones, which overlie the Guimal sandstones. Using a deposition depth at the shallow end of the uncertainty range for this unit would give a much smoother form to the tectonic subsidence and reduced subsidence during Guimal deposition. Overestimation of the subsidence during deposition of the Guimal Formation may also arise from decompacting the predominantly sandy unit to unrealistically high porosity values. There is some evidence that a renewed extensional phase may have affected the continental margin in the early Cretaceous. Influx of trachytic volcanic rock fragments in the Albian (Gaetani & Garzanti 1991) may derive from intra-plate volcanism related to extension. The timing also coincides with the rifting of India from Africa and Madagascar to the west, and from Australia to the east, and with final opening of the Indian Ocean.

#### *Mid- to Late Cretaceous*

Following the deposition of the Guimal sandstones, there is a pronounced difference in the form of the subsidence curves based on the Watts & Steckler (1979) sea-level curve for the two sections. In the Zangla section, during deposition of the Chikkim Formation and the Kangi La Formation there appears to be slight tectonic uplift. This is irrespective of which sea-level curve is used (Fig. 4a). Because each of these formations was deposited in deep water the potential for recording tectonic uplift is good. Although potential uncertainties, particularly the depth of deposition, prevent exact interpretation, it is certainly the case that there was little or no subsidence during this period of time in the Zangla section. This confirms the observations of Premori Silva *et al.* (1991), who suggested that the lack of any subsidence associated with deposition of the Kangi La Formation ruled out the possibility of a flexural, syn-ophiolite obduction origin (Searle 1986). However, the Zangla section represents the more proximal parts of the passive margin. The subsidence rate recorded in relatively distal parts of the margin by the Yulchung section is very different. A rapid subsidence rate is associated with deposition of the Fatu La Formation and in particular the Kangi La Formation, with a total of 200–300 m subsidence recorded over this time period. Once again, this trend is observed regardless of which sea-level curve is used (Fig. 5b). This inferred subsidence is sufficiently large to be robust to the uncertainties that have been discussed in decompaction and the formation thicknesses. As a result of the shaly or micritic nature of these formations the decompaction estimates are likely to be minimum estimates, suggesting that subsidence could in fact be considerably greater.

There is no evidence for a further stretching phase to cause this subsidence. Therefore, in sharp contrast to the Zangla section, the Yulchung section does appear to require some additional tectonic mechanism to account for the increase in subsidence rate. The most likely source of this subsidence is

flexure of the leading margin of the Indian plate outboard of the continental shelf by the thrust load of the Spontang ophiolite. The youngest sediments in the distal Karamba complex within the Indus Suture Zone are Campanian (Robertson & Sharp 1988), which suggests that thrusting occurred during the Late Cretaceous.

#### *Flexure caused by ophiolite loading*

One explanation for the reduced subsidence and possible uplift of the relatively proximal Zangla section and the subsidence of the Yulchung section is flexural loading of the north-facing Indian continental margin by the Spontang ophiolite. To test this possibility, we have determined the flexure associated with an elastic plate overlying an inviscid substratum that is subject to arbitrary-shaped 2D end loads and compared it with the tectonic subsidence and uplift deduced from backstripping at Zangla and Yulchung.

On the basis of the cross-sections of Corfield & Searle (2000), the restored distance between the position of the leading edge of the Spontang ophiolite and associated Neo-Tethyan thrust sheets and the Indus Suture Zone is calculated as 70 km. This distance is therefore a measure of the minimum distance the Spontang ophiolite was obducted onto the north-facing Indian margin. Because mantle rocks are exposed at the base of the Spontang ophiolite (Reuber 1986; Corfield *et al.* 2001), and assuming a typical oceanic crust structure, the obducted sheet must have been at least 5 km thick and probably thicker. These estimates provide the best constraints, we believe, for the shape of the load that would result from the obduction of the Neo-Tethyan thrust sheets onto the continental margin. The load has therefore been modelled as a 70 km wide triangular wedge tapering from 10 km thick to 0 km at the leading edge. The flexure of the plate has been calculated for a range of  $T_c$  values, an infill load of water, and a 'driving' load that displaces either water or air (Fig. 7).

The calculations in Figure 7 are based on a discontinuous (i.e. broken), rather than a continuous, elastic plate. In our mapped region, there is no obvious plate break along the Indian margin south of the Indus Suture Zone. However, during the mid- to late Cretaceous the north Indian margin was entering a subduction zone beneath the overriding thrust load (Searle *et al.* 1997; Corfield *et al.* 1999). The broken plate model has been widely used at present-day subduction zones (Hanks 1971) and we believe that it is a reasonable approximation to the mechanical behaviour of the Indian margin, at least during the stage when the margin is being subducted.

#### **Discussion**

We assumed in the calculations in Figure 7 that water infills the flexural depression and, hence, that the obducted ophiolite load will 'fall in' and occupy part of the flexure. The load remains largely or even entirely below sea level in the case of values of a weak foreland with  $T_c$  in the range of 5–10 km. This is true irrespective of whether the 'driving' ophiolite load displaces water or air. The load height increases, however, with higher values of the elastic thickness, as does the distance from the front of the load to the crest of the peripheral bulge, and width and height of the peripheral bulge.

Evidence of the depositional truncation of the Yulchung thrust by early Tertiary limestones (Corfield & Searle 2000) suggests that the leading edge of the obducted thrust sheets reached the area of the Yulchung section at this time. This, together with the slight tectonic uplift at the Zangla section (SW) and subsidence

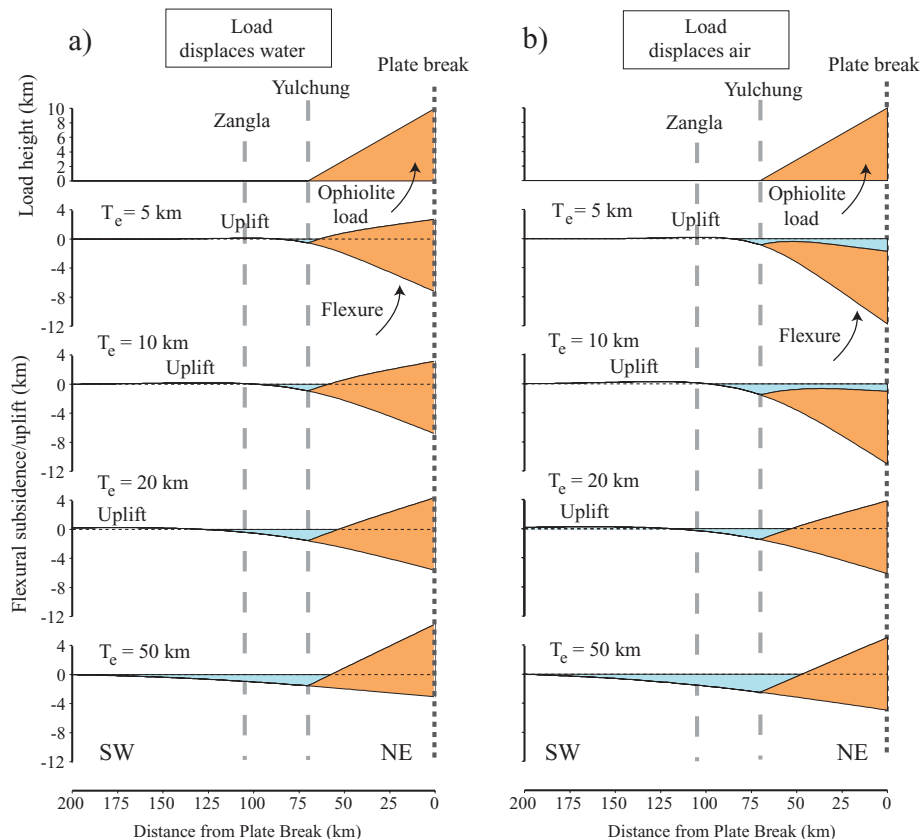


**Fig. 7.** Simple model of flexure for the loading of a passive margin by an obducted ophiolite. The calculations are based on a discontinuous (i.e. broken) elastic plate model, a 70 km wide wedge-shaped load that tapers from 10 km to 0 km thick, a load and mantle density of  $2700 \text{ kg m}^{-3}$  and  $3330 \text{ kg m}^{-3}$ , respectively, and  $T_e$  values of 5, 10, 20 and 50 km. Two cases of loading are shown, according to whether the ophiolite displaces water (a) or air (b). All models assume that water of density  $1030 \text{ kg m}^{-3}$  infills the depression and, hence, that the obducted ophiolite load will “fall in” and occupy part of the flexure. The exaggerated vertical scale should be noted. The model is representative of the obduction of the Spontang ophiolite (load) onto the Indian continental margin (broken elastic plate).

at the Yulchung section (NE) during the late Cretaceous, provide important constraints on the flexure model.

Figure 7 shows that the best fit to the uplift and subsidence patterns at Zangla and Yulchung is for flexural loading models based on  $T_e$  of 5–10 km. Models based on higher values of  $T_e$  (e.g. 20 km) predict a wide foreland basin, and subsidence rather than uplift at Zangla. Furthermore, the small subaerial exposure of the load in the models based on  $T_e$  of 5–10 km is consistent with the lack of any significant erosional debris from the ophiolite during the proposed late Cretaceous obduction.

The best fit flexure models imply a subsidence immediately in advance of the ophiolite of *c.* 0.9–1.5 km, which is somewhat larger than observed in the backstripped section. However, the predicted values assume sharp, geometric shapes for the load. In reality, several thrust sheets are obducted, each of which is deformed internally by further folding and thrusting. The leading thrust slices are likely to comprise material with a lower density than the  $2600 \text{ kg m}^{-3}$  that we have assumed for the ophiolite load and therefore the subsidence at the front of the thrust sheet has probably been overestimated.

So far, we have considered the load only in its final resting place. In fact, the ophiolite load would have been added progressively such that the accompanying flexural depression and flanking bulge would have migrated SW across the north-facing Indian margin at approximately the same rate as the obduction. Unfortunately, because of the high degree of deformation and lack of continuity of the shelf succession SW of the High Himalaya, it is difficult to resolve any bulge migration across the Yulchung section. However, a progressive flexural loading model is supported by a clear lithological change in the Kangi La Formation from Zangla to Yulchung. In addition to a thickening of the formation from 500 m to over 1 km the regular bedded

character in the Zangla area becomes much more disturbed, with major slump features in the Yulchung area, consistent with a flexural slope. Any migration of a bulge in the Yulchung area may be recorded in the detailed stratigraphy of the lower Kangi La Formation, but this is beyond the scope of the data available for this work.

Although our flexural modelling is clearly simplified, it does illustrate, we believe, that the observed tectonic subsidence and uplift pattern deduced from backstripping is entirely consistent with a late Cretaceous obduction event. Other well-studied ophiolites such as in Oman also show emplacement into and on top of a rapidly subsiding foreland (e.g. Patton & O’Connor 1988) and never directly onto shallow marine limestones, as required if the Spontang ophiolite was obducted in the Tertiary.

#### *Elastic thickness*

In the oceans,  $T_e$  depends strongly on the thermal age of the lithosphere at the time of loading (Watts 1978). There is evidence that when oceanic lithosphere is reheated, for example, as a result of ‘hotspot’ volcanism,  $T_e$  is reset to lower values (Calmant & Cazenave 1987) and subsequently rises with time as the plate cools. The thermal and mechanical behaviour of continental lithosphere, however, is not as well understood. Although it has been proposed (Karner *et al.* 1983) that continental  $T_e$  also depends on the age of the lithosphere at the time of loading, there is no evidence that, in the case of rift-type basins in continental margins, sediments emplaced during the later stages of their evolution are supported by a lithosphere that has recovered its strength with time. Indeed, the published  $T_e$  estimates from rift-type basins are low and they appear to remain low after rifting.

The rifting event that preceded north Indian passive margin formation came to an end at around 220 Ma, 120–150 Ma before the emplacement of the Spontang ophiolite loading event. The best example, perhaps, of where a large load has been emplaced on a passive margin is Taiwan. Here, thrust and fold loading of a Palaeogene (*c.* 38–50 Ma) margin created a foreland basin, the basal sequence of which is dated at *c.* 6.5 Ma. The  $T_c$  derived at this foreland of 13 km (Lin & Watts 2002) is therefore representative of extended continental lithosphere, *c.* 31–43 Ma after a rifting event.

Global compilations of  $T_c$  from foreland basins suggest, however, a bimodal distribution with peaks at 10–20 km and 80–90 km. Watts (1992) suggested that this distribution was caused by the diversity in the structural fabric of thrust and fold loading, with some loads being limited to weak extended lithosphere whereas others were able to ‘telescope’, across the passive margin hinge zone and onto strong cratonic lithosphere.

The flexure model applied to the Zanskar passive margin considers only the effects of vertical loads. The model therefore ignores the effects of any horizontal loads that might arise as a consequence of ophiolite emplacement. As Cloetingh (1986), Karner (1986) and others have shown, tectonic boundary loads at compressional plate boundaries increase the curvature and, hence, reduce the  $T_c$  of the subducting lithosphere from what it might otherwise be in the absence of such loads. However, even in the absence of tectonic boundary loads, ophiolite obduction imposes significant stresses on the flexed plate. The Spontang ophiolite, for example, is associated with partial subduction of buoyant continental crust. Therefore, significant compressive forces are likely during ophiolite emplacement. This is confirmed by the D<sub>1</sub> (late Cretaceous) phase of regional shortening (Searle 1986; Corfield & Searle 2000). Horizontal compressive forces and significant bending of the loaded plate suggest therefore the possibility that the  $T_c$  that we have deduced at the north Indian margin might be unusually low and that the actual  $T_c$  of the underlying lithosphere may be higher.

Thrusting of the proximal to distal Lamaywu and Karamba complex thrust sheets onto the passive margin occurred during the Late Cretaceous (post-Campanian). These thrust sheets together with the highest Spontang ophiolite loaded the Indian passive margin, which flexed down to accommodate the emplacing thrust sheets.

The only other case that we are aware of where  $T_c$  has been estimated at an ophiolite-loaded rifted margin is Oman. Patton & O’Connor (1988), for example, have used the geometry of the foreland basin, created by the emplacement of the Oman ophiolite on the Arabian margin during the mid-Cretaceous, to estimate a  $T_c$  of *c.* 15 km. The Aruma foredeep basin in Oman developed by flexure of the Arabian plate margin in front of and beneath the emplacing Semail ophiolite thrust sheet.

### Early Tertiary

After ophiolite obduction in the late Cretaceous, each of the restored sections shows a low rate of subsidence. This is most apparent during the deposition of the Palaeocene–Eocene shallow marine limestones in Ladakh. We attribute this low rate to the continued post-rift thermal subsidence of the Indian margin.

Several geological factors further support the model of late Cretaceous obduction by the Spontang ophiolite. The shelf carbonate sequence beneath the ophiolite shows numerous thrusts and tight to isoclinal folds, which are truncated by the base-Tertiary unconformity. The overlying Palaeocene–Eocene limestones are only gently folded, showing that a major phase of

crustal shortening must have occurred during the late Cretaceous (Searle 1986; Searle *et al.* 1988, 1997). The youngest marine sediments on the Indian continental margin and at the Indus Suture are early Eocene (54–50 Ma), indicating the minimum age of the India–Asia collision. Continued shortening followed the early Eocene sedimentation and resulted in renewed compressional folding and break–back thrusting. It was this late phase of thrusting that placed the Spontang ophiolite over Eocene limestones in Zanskar.

### Conclusions

The subsidence history of the Indian continental margin in the Zanskar region can be modelled in terms of several distinct tectonic events. Rifting initiated at 270 Ma associated with the eruption of the Panjal volcanic rocks, with a subsequent subsidence history of the newly formed passive margin comparing very well with theoretical models. For a typical initial crustal thickness of 31.2 km, minimum  $\beta$  estimates of *c.* 1.2 have been obtained for relatively proximal and distal locations, respectively.

In the late Cretaceous, uplift of the innermost margin and rapid subsidence in the more distal Yulchung section have been documented. These tectonic movements are interpreted as the flexural response of the north-facing Indian continental margin to ophiolite obduction. The backstrip data compare well with the predictions of a broken elastic plate model that is loaded by a 70 km wide wedge-shaped load tapering from 10 to 0 km thick. The  $T_c$  that best fits the uplift (and subsidence) data is in the range of 5–10 km.

After obduction, there was a slow rate of subsidence, which reflects the continuing cooling of the underlying Indian lithosphere after rifting. Structural and stratigraphic data show that a major phase of crustal shortening occurred during the late Cretaceous before the deposition of shallow-marine Palaeocene to early Eocene limestones.

The successful application of the backstripping technique, which was developed for modern passive margins, to a highly deformed fold and thrust belt is perhaps surprising. However, there are several features of the Zanskar passive margin that have contributed to this success. Most notably, the stratigraphy preserves a remarkably continuous sedimentation throughout the Mesozoic, with no major unconformities associated with periods of non-deposition. This is perhaps most significant in the late Cretaceous, when high sea levels and deep-water conditions before ophiolite obduction meant that the flexural loading event probably was initiated below, rather than above, sea level.

This work was carried out with NERC (UK) grants to R.I.C. (GT4/95/247/E) and M.P.S. (GT5/96/13/E). We are grateful to O. Green and R. Bisley for field assistance, to F. H. Mitoo for logistical support, and to J. Stewart for help with the backstripping calculations. We thank A. Robertson and A. Smith for their critical review and helpful comments.

### References

- BOND, G.C. & KOMINZ, M.A. 1984. Construction of tectonic subsidence curves for the early Paleozoic Miogeocline, southern Canadian Rocky Mountains: implications for subsidence mechanisms, age of breakup and crustal thinning. *Geological Society of America Bulletin*, **95**, 155–173.
- CALMANT, S. & CAZENAVE, A. 1987. Anomalous elastic thickness of the oceanic lithosphere in the south–central Pacific. *Nature*, **32**, 236–238.
- CLIFT, P.D., TURNER, J. & LEG 152 SCIENTIFIC PARTY, 1995. Dynamic support by the Icelandic plume and vertical tectonics of the northeast Atlantic continental margins. *Journal of Geophysical Research*, **100**, 24473–24486.
- CLOETINGH, S. 1986. Intraplate stresses: a new tectonic mechanism for relative fluctuations of sea level. *Geology*, **14**, 617–620.

- COCHRAN, J.R. 1981. Simple models of diffuse extension and the pre-sea-floor spreading development of the continental margin of the northwestern Gulf of Aden. *Oceanologica Acta*, Proceedings of the 26th International Geological Congress, Geology of Continental Margins Symposium, Paris, July 7–17, 1980, 154–165.
- COCHRAN, J.R. 1983. Effects of finite extension times on the development of sedimentary basins. *Earth and Planetary Science Letters*, **66**, 289–302.
- COLCHEN, M., REUBER, I., BELLIER, J.-P., BLONDEAU, A., LYS, M. & WEVER, P.D. 1987. Données biostratigraphiques sur les mélanges ophiolitiques du Zaskar, Himalaya du Ladakh. *Comptes Rendus de l'Académie des Sciences, Série II*, **305**, 403–406.
- CORFIELD, R.I. & SEARLE, M.P. 2000. Crustal shortening estimates across the north Indian continental margin, Ladakh, NW India. In: KHAN, M.A., TRELOAR, P.J., SEARLE, M.P. & JAN, M.Q. (eds) *Tectonics of the Nanga Parbat Syntaxis and the Western Himalaya*. Geological Society, London, Special Publications, **170**, 395–410.
- CORFIELD, R.I., SEARLE, M.P. & GREEN, O.R. 1999. Photang thrust sheet—an accretionary complex structurally below the Spontang ophiolite constraining timing and tectonic environment of ophiolite obduction, Ladakh Himalaya. *Journal of the Geological Society, London*, **156**, 1031–1044.
- CORFIELD, R.I., SEARLE, M.P. & PEDERSON, R.B. 2001. Tectonic setting, origin and obduction history of the Spontang Ophiolite, Ladakh Himalaya, NW India. *Journal of Geology*, **109**, 715–736.
- GAETANI, M. & GARZANTI, E. 1991. Multicyclic history of the northern India continental margin (north-western Himalaya). *AAPG Bulletin*, **75**, 1427–1446.
- GAETANI, M., GARZANTI, E. & TINTORI, A. 1990. Permo-Carboniferous stratigraphy in SE Zaskar and NW Lahul (NW Himalaya, India). *Eclogae Geologicae Helveticae*, **83**, 143–161.
- GARZANTI, E., BAUD, A. & MASCLE, G. 1987. Sedimentary record of the northward flight of India and its collision with Eurasia (Ladakh Himalaya, India). *Geodinamica Acta*, **1**, 297–312.
- HANKS, T.C. 1971. The Kuril trench–Hokkaido rise system: large shallow earthquakes and simple models of deformation. *Geophysical Journal of the Royal Astronomical Society*, **23**, 173–189.
- HAQ, B.U., HARBENBOL, J. & VAIL, P.R. 1987. Chronology of fluctuating sea levels since the Triassic. *Science*, **235**, 1156–1167.
- HONEGGER, K., DIETRICH, V., FRANK, W., GANSSER, A., THONI, M. & TROMMSDORF, V. 1982. Magmatism and metamorphism in the Ladakh Himalayas (the Indus–Tsangpo suture zone). *Earth and Planetary Science Letters*, **60**, 253–292.
- JARVIS, G.T. & MCKENZIE, D.P. 1980. Sedimentary basin formation with finite extension rates. *Earth and Planetary Science Letters*, **48**, 42–52.
- KARNER, G.D. 1986. Effects of lithospheric in-plane stress on sedimentary basin stratigraphy. *Tectonics*, **5**, 573–588.
- KARNER, G.D., STECKLER, M.S. & THORNE, J. 1983. Long-term mechanical properties of the continental lithosphere. *Nature*, **304**, 250–253.
- KELEMAN, P.B. & SONNENFELD, M.D. 1983. Stratigraphy, structure, petrology and local tectonics, Central Ladakh, NW Himalaya. *Schweizerische Mineralogische und Petrographische Mitteilungen*, **63**, 267–287.
- LIN, A.T. & WATTS, A.B. 2002. Origin of the West Taiwan basin by orogenic loading and flexure of a rifted continental margin. *Journal of Geophysical Research*, **107**, 10.1029/2001JB000669.
- MCKENZIE, D.P. 1978. Some remarks on the development of sedimentary basins. *Earth and Planetary Science Letters*, **40**, 25–32.
- MCKENZIE, D.P. & BICKLE, M. 1988. The volume and composition of melt generated by extension of the lithosphere. *Journal of Petrology*, **29**, 625–679.
- PATTON, T.L. & O'CONNOR, S.J. 1988. Cretaceous flexural history of northern Oman mountain foredeep, United Arab Emirates. *AAPG Bulletin*, **72**, 797–809.
- PEDERSON, R., SEARLE, M.P. & CORFIELD, R.I. 2001. U–Pb zircon ages from the Spontang Ophiolite, Ladakh Himalaya. *Journal of the Geological Society, London*, **158**, 513–520.
- PITMAN, W.C. 1978. The relationship between eustasy and stratigraphic sequences of passive margins. *Geological Society of America Bulletin*, **89**, 1389–1403.
- PREMORI SILVA, I., GARZANTI, E. & GAETANI, M. 1991. Stratigraphy of the Chikkim and Fatu La formation in the Zangla and Zumlung units (Zaskar Range, India) with comparisons to the Thakkola region (Central Nepal): Mid-Cretaceous evolution of the Indian passive margin. *Rivista Italiana di Paleontologia e Stratigrafia*, **97**, 511–564.
- REUBER, I. 1986. Geometry of accretion and oceanic thrusting of Spontang ophiolite, Ladakh-Himalaya. *Nature*, **321**, 592–596.
- ROBERTSON, A. & SHARP, I. 1988. Mesozoic deep-water slope/rise sedimentation and volcanism along the North Indian passive margin: evidence from the Karamba complex, Indus suture zone (western Ladakh Himalaya). *Journal of Asian Earth Sciences*, **16**, 195–215.
- SEARLE, M.P. 1986. Structural evolution and sequence of thrusting in the High Himalayan, Tibetan–Tethys and Indus suture zones of Zaskar and Ladakh, Western Himalaya. *Journal of Structural Geology*, **8**, 923–936.
- SEARLE, M.P., COOPER, D.J.W. & REX, A.J. 1988. Collision tectonics of the Ladakh–Zaskar Himalaya. *Philosophical Transactions of the Royal Society of London, Series A*, **326**, 117–150.
- SEARLE, M.P., CORFIELD, R.I., STEPHENSON, B.J. & MCCARRON, J. 1997. Structure of the north Indian continental margin in the Ladakh–Zaskar Himalayas: implications for the timing of obduction of the Spontang ophiolite, India–Asia collision and deformation events in the Himalaya. *Geological Magazine*, **134**, 297–316.
- VAIL, P.R., MITCHUM, R.M. & THOMPSON, S. 1977. Relative sea-level from coastal onlap. In: PAYTON, C.E. (ed.) *Seismic Stratigraphy—Applications to Hydrocarbon Exploration*. American Association of Petroleum Geologists, Memoirs, **26**, 63–82.
- WATTS, A.B. 1978. An analysis of isostasy in the world's oceans: I. Hawaiian–Emperor Seamount Chain. *Journal of Geophysical Research*, **83**, 5989–6004.
- WATTS, A.B. 1992. The effective elastic thickness of the lithosphere and the evolution of foreland basins. *Basin Research*, **4**, 169–178.
- WATTS, A.B. & RYAN, W.B.F. 1976. Flexure of the lithosphere and continental margin basins. *Tectonophysics*, **36**, 25–44.
- WATTS, A.B. & STECKLER, M.S. 1979. Subsidence and eustasy at the continental margin of eastern North America. In: TALWANI, M., HAY, W. & RYAN, W.B.F. (eds) *Deep Drilling Results in the Atlantic Ocean: Continental Margins and Paleoenvironment*. American Geophysical Union, Maurice Ewing Series, **3**, 218–234.
- WOOLER, D.A., SMITH, A.G. & WHITE, N. 1992. Measuring lithospheric stretching on Tethyan passive margins. *Journal of the Geological Society, London*, **149**, 517–532.